

## ON THE POSSIBILITY OF EVAPORATOR DRASTIC SCALE REDUCTION IN A PERIODICALLY OPERATING TWO-PHASE THERMOSYPHON

S. Filippeschi, E. Latrofa, G. Salvadori

Department of Energetic "Lorenzo Poggi"  
University of Pisa  
s.filippeschi@ing.unipi.it

### ABSTRACT

In order to use a Periodically operating Two-Phase Thermosyphons (PTPT) in microelectronic equipment cooling, the possibility of a drastic reduction in the scale of the evaporator is considered. In previous studies a miniature PTPT was realised with an internal volume of  $352 \times 10^{-6} \text{ m}^3$  and an evaporator volume of  $238 \times 10^{-6} \text{ m}^3$ .

It has shown thermal resistance similar to other unsteady wickless two phase devices as PHPs. The present paper reports an experimental study on the minimum volume of working fluid, which is necessary to obtain a stable operating mode. Our experiments, carried out with FC-72 as working fluid, have shown that the PTPT works in a stable heat transport regime even when the working fluid transported volume is about  $3 \times 10^{-6} \text{ m}^3$ . The maximum wall temperature stays below  $100 \text{ }^\circ\text{C}$  till a heat flux of  $16.2 \times 10^4 \text{ W/m}^2$  is reached. Nevertheless, by keeping the heat flux constant and decreasing the volume of working fluid transported, an increase in total thermal resistance is obtained. This increase rate is, however, small — lower than 25% if the volume of working fluid transported is reduced from 64 to  $3 \times 10^{-6} \text{ m}^3$ .

### INTRODUCTION

High heat fluxes and small heating surfaces make the use of two phase devices with natural circulation necessary, above all in electronic and microelectronic equipment cooling. The two-phase heat transfer devices with natural circulation that are investigated nowadays can be divided into two main groups: capillary driven and thermally driven.

The first group consists of heat pipes, LHPs and CPLs [1], [2] which are those most frequently investigated and are used in low gravity conditions [3]-[4]. They are characterised by good thermal performances that are not greatly influenced by the evaporator orientation with respect to gravity or by the location of the evaporator with respect to the condenser. But they have also high manufacturing costs because the capillary structure of the evaporators can only be implemented by using advanced technologies. At the moment, however, these seem to be the most adequate for micro-cooling devices [5].

The second group comprises loop thermosyphons, which work in a steady state heat transfer mode and Pulsating Heat Pipes (PHPs) or Periodically operating Two Phase Thermosyphons (PTPTs), which works with an unsteady state heat transfer regime. In general they have low manufacturing costs because they are wickless devices. Devices in the second group have lower thermal resistances than the capillary driven loops, but their performance is usually influenced by gravity.

Some studies on mini two-phase loop thermosyphons are reported in [6], [7]. Their usefulness as a micro-cooling device may be limited by the low static pressure head that makes the working fluid circulation unstable if the internal diameter of the connecting pipes is lower than 4 mm [8].

On the other hand thermally driven devices with unsteady heat transport seem to be less influenced by gravity and high pressure drops, and they are therefore the most adequate

wickless applications in micro heat transfer conditions, and the most investigated unsteady wickless devices are, at the moment, the PHPs [9]-[10]. Groll et al. [11] have presented a single turned PHP with an evaporator section of size  $40 \times 30 \times 5 \text{ mm}^3$  that has operated efficiently using tubes with an internal diameter of 2 mm and a tilt angle of up to  $10^\circ$ ; the working fluid has been methanol. They have seen that the thermal resistances increase from 1.07 to 3.7 W/K as the power input decreases from 74.4 to 14.8 W/K, with the PHP operating in a vertical mode (190 mm is the level difference between condenser and evaporator). They have seen that a stable regime is hard to obtain if the PHP operates in horizontal mode. Rittidech et al. [12] have tested several inner diameters (0.66, 1.06 and 2.03 mm) and different fluids (R123, ethanol, water) in a PHP with the same length of the evaporating and condensing section. This PHP has operated in horizontal mode but the maximum heat flux removed is only about  $0.7646 \times 10^4 \text{ W/m}^2$ .

Other devices operating with unsteady heat transfer regime are less well known and have only been rarely investigated. Some devices characterized by a periodic heat transfer regime have been named Pulsated Two-Phase Thermosyphons by the present authors in [13]-[16] but are better characterised by the name Periodically operating Two-Phase Thermosyphons.

They are loop thermosyphons where an accumulation volume is inserted in the liquid line and two check valves are present in the loop. The circulation of the fluid is generated by periodic pressure oscillations that can be produced naturally or forcedly. In the first case they occur because of the emptying of the liquid in the evaporator while in the second case they are due to the periodic opening and closing of valves. The PTPT device can operate with the condenser positioned at any sites with regard to the evaporator. One of the first PTPTs was presented by Tamburini [17] in 1977 for electronic cooling in spatial applications, but more recently many similar devices have been applied to

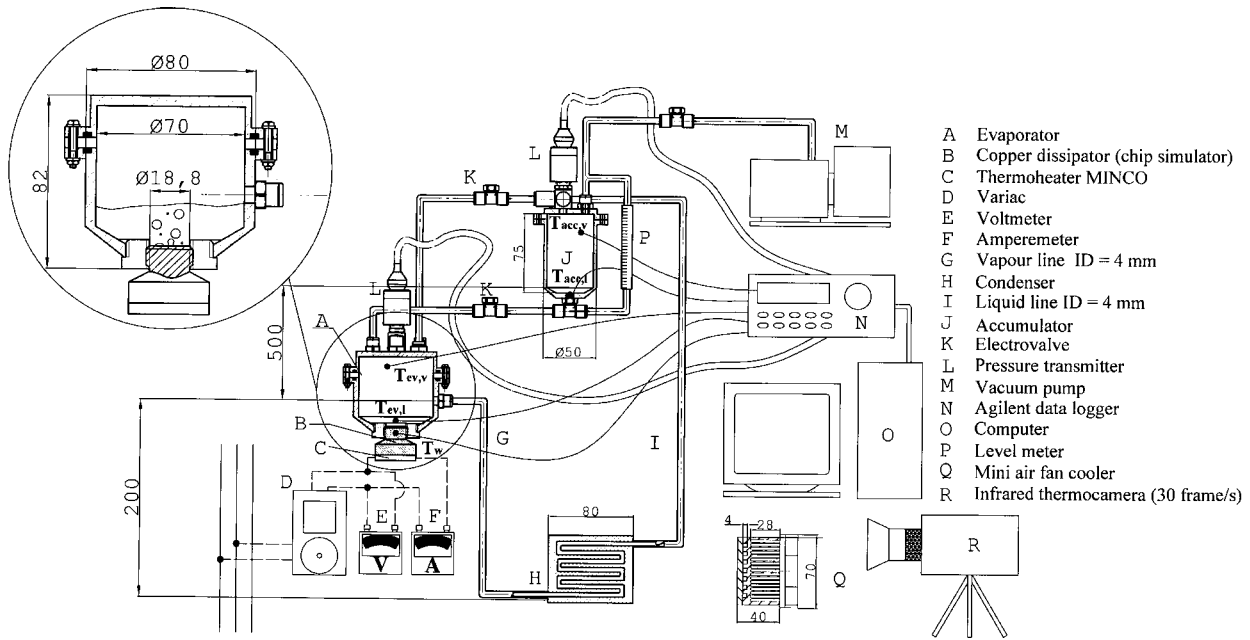


Fig 1: Experimental set up (All the dimensions are in mm)

different fields (see, for instance, [18]-[19]). However, all the devices tested are large in size, as is one of the PTPTs that has recently been experimentally investigated [13] and numerically simulated [14] by the present authors. It has an evaporator with a volume of about  $0.012 \text{ m}^3$  which is placed 1 m over the condenser. Using HCFC 141 b as working fluid, an input power of 1200 W has been dissipated with a thermal resistance of about  $0.5 \text{ K/W}$ . In order to apply a PTPT device in microelectronic equipment cooling a new experimental apparatus has been implemented [20]. The size of the new device has been drastically reduced so that it is, at the moment, contained in a case for a desktop computer with an evaporator whose internal volume is about  $238 \times 10^{-6} \text{ m}^3$ . The mini PTPT device has shown good thermal performances, and thermal resistances similar to PHP ones. Moreover, a stable operating mode has been observed whether the condenser is placed over or under the evaporator. The temperatures of the evaporator heating surface are lower than  $100 \text{ }^\circ\text{C}$  and the heat flux removed is about  $9.55 \times 10^4 \text{ W/m}^2$  with FC72 as working fluid [20]. These results seem to encourage further investigation, but in order to use a PTPT device in microelectronic cooling the evaporator size must be drastically reduced to values similar to those for the flat evaporators used in the recent micro heat pipes [21]-[22], in all cases lower than  $40 \times 10^{-6} \text{ m}^3$ . The minimum volume of the evaporator is linked to the minimum volume of working fluid transferred in every cycle. This paper presents some experiments on the minimum volume of working fluid necessary to obtain a stable operating mode in PTPT device. The experiments have been carried out by increasing the power input to  $45 \text{ W}$  (heat flux  $16.2 \times 10^4 \text{ W/m}^2$ ).

## EXPERIMENTAL FACILITY

### Test apparatus

The tested PTPT loop consists of 3 main components: evaporator (internal volume  $238 \times 10^{-6} \text{ m}^3$ ), condenser ( $10 \times 10^{-6}$

$\text{m}^3$ ) and accumulator ( $70 \times 10^{-6} \text{ m}^3$ ). They are connected in a loop with different lines ( $34 \times 10^{-6} \text{ m}^3$ ) as shown in Fig. 1.

The evaporator volume is 67% of the total PTPT volume ( $352 \times 10^{-6} \text{ m}^3$ ). The condenser, air cooled by a fan, is made of an aluminium plate  $64 \times 78 \times 8 \text{ mm}^3$  with 22 rectangular fins, 28 mm high, 78 mm long and 1.3 mm thick. Inside the plate a serpentine groove with a  $4 \times 4 \text{ mm}^2$  section surface has been manufactured. All the connection lines are flexible polyethylene pipes with an internal diameter of 4 mm. The check valves are small (35 mm long, with an external diameter of about 15 mm), while the stainless steel solenoid valves are of 2 way type, normally closed with an opening response time of 5 ms.

The electronic component is simulated by a cylindrical copper dissipator heated by a thermo-heater. The heating surface  $S$  wetted by the working fluid is  $2.77 \times 10^{-4} \text{ m}^2$ , as can be understood from the evaporator and dissipator section reported in Fig. 1. A ring made of PTFE thermally disconnects the copper dissipator from the aluminium case of the evaporator. The working fluid is FC72.

### Control system and data acquisition

The control system consists of a digital timer (0.01 s to 1000 hours), covering various operational modes. In the experiments it is set with a time where the valves are off ( $\Delta\tau_1$ ) and a time where the valves are on ( $\Delta\tau_2$ ).

The temperature of the plane heating surface  $T_w$  is measured by a K-type thermocouple 0.5 mm thick. It is located 2 mm under the surface of the copper dissipator. All the thermocouples are of K-type, 1 mm thick, and measure the following temperatures: temperature of liquid pool close to the heating surface  $T_{ev,l}$ , the saturation temperature of the vapour  $T_{ev,v}$  inside the evaporator, the temperatures of the collected liquid  $T_{acc,l}$  and the saturation temperature of the vapour  $T_{acc,v}$  inside the accumulator.

All the external surfaces of the components have been covered with a film of known emittance ( $\epsilon = 0.95$ ) which

make it possible to measure all the temperatures of the loop with an infrared thermo camera. The vapour pressures of accumulator and evaporator are measured by a Druck PTX 75-11 transmitter (0 to 2.5 bar, accuracy 0.25% of full scale range). A level meter is inserted in the accumulator. All the temperatures and pressures within the device are sampled by a data acquisition system Agilent 34970A (thermal resolution 0.1 °C, accuracy  $\pm 0.5$  °C, minimum acquisition frequency 3 Hz) and stored in a PC microcomputer (experimental scanning time step 3 s).

The volume  $V_T$  of working fluid transferred in every cycle has been measured by a level meter located inside the accumulator: its accuracy is about  $\pm 0.76 \times 10^{-6}$  m<sup>3</sup>.

### PTPT operational mode

The operational mode of a generic PTPT is described in [13]-[16] and is quickly summarized here.

The evaporator is continuously heated by power input  $Q$ , while the condenser and the accumulator are cooled by two different sources at constant temperatures — a low one  $T_C$  and an intermediate one  $T_m$ . Usually the temperatures of the cold source and the intermediate source are the same because the two elements are inserted in the same environment. The power rate dissipated by the condenser  $Q_C$  and the accumulator  $Q_m$  depend on time, while the power input  $Q$  is constant. The heat dissipated by the connecting lines is negligible. The relative position of condenser and evaporator weakly influences the thermal behaviour of the device [8].

There are different kinds of PTPT [13]-[16], but the PTPT used in this study operates in the following way.

At the starting time all the liquid is in the evaporator. As the power input is supplied, the liquid increases its temperature and pressure and starts to evaporate. The volume of the liquid pool  $V_{ev,l}$  therefore varies over time. The vapour goes into the condenser, where it is condensed and subcooled. A column of liquid between the condenser and evaporator is created in this way.

The pressure inside the evaporator increases, so lifting the liquid column from the condenser to the accumulator. As the condensed liquid reaches the accumulator, the pressure and temperature inside the evaporator stop to increase and a constant liquid mass flow rate is observed.

The pressure and temperature  $p_{ev,v}$  and  $T_{ev,v}$  remain almost unchanged during this period [14], but as soon as a given volume  $V_T$  of working fluid is transferred from the evaporator to accumulator, the electrovalves open the connecting lines between evaporator and accumulator. The accumulated cold liquid returns to the evaporator, the heat transfer cycle is closed and all the operations repeat themselves again. After some few cycles the device reaches a stable regime [20]. The temperature of the working fluid inside the evaporator and accumulator during a single heat transfer cycle are shown in Fig. 2.

The heat transfer period of a single cycle can be divided into two main parts: time difference  $\Delta\tau_1$  with electrovalves off and time difference  $\Delta\tau_2$  with electrovalves on, which is also the time required for the return of the liquid into the evaporator. Moreover, the time difference  $\Delta\tau_1$  can be itself divided into two parts. In the first ( $\tau_r - \tau_0$ ), the vapour is compressed according to an isovolumic operation [16], while in the second part ( $\tau_l - \tau_r$ ), the liquid is transported from the evaporator to the accumulator [16]. Temperatures, pressures and mass flow rate are approximately constant during the time

difference ( $\tau_l - \tau_r$ ), while are changing during the remaining time of the cycle. On the other hand the volume of the liquid inside the evaporator is constant during the time difference ( $\tau_l - \tau_0$ ), while it is changing in the remaining time of the cycle.

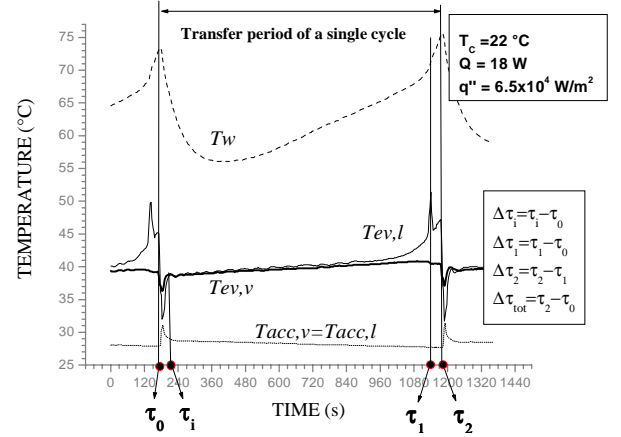


Fig. 2: Temperature trends during a single PTPT heat transfer cycle as a stable regime is reached.

One of the technical parameters that can describe the thermal behaviour of a PTPT is its thermal resistance.

The definition of thermal resistance for a PTPT is different from that of a classical thermosyphon, firstly because PTPT is a device that dissipates heat with two heat sinks at different temperatures, and secondly because all the temperatures of the working fluid are depend periodically on time. The following theoretical treatment is not completely exact, because some heat transfer phenomena can not be expressed by a linear relation or because it is not possible to associate a thermal resistance with a heat transfer regime. The following treatment, however, is useful to well understand which main phenomena influence the heat transfer in a such device.

If only the period taken for a mass to be transported from evaporator to accumulator ( $\tau_l - \tau_r$ ) is considered, it is possible to describe the thermal behaviour of a generic PTPT by means the schematic diagram shown in Fig. 3. In fact, during this period, which represents most of the heat transfer cycle time, the temperatures inside the loop remain unchanged and the unsteady behaviour of the device is irrelevant.

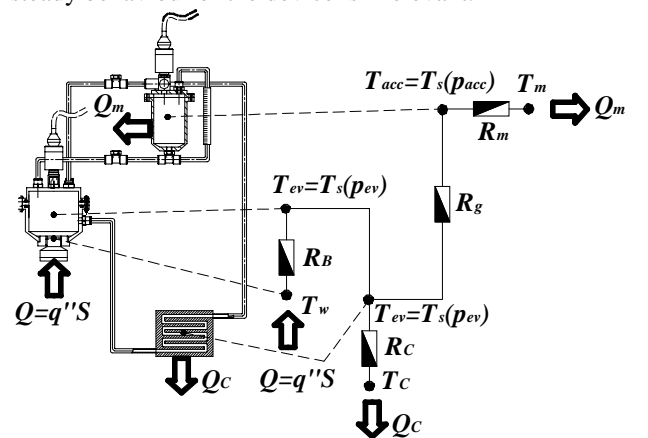


Fig. 3: Thermal resistances of a PTPT

With reference to Fig. 3, if the heat losses from the vapour and liquid lines are negligible, it is possible to individuate the following thermal resistances:  $R_B$  is the thermal resistance connected with the heat transfer regime between the heating surface and the working fluid, which is usually a boiling

regime, while  $R_C$  and  $R_m$  are the thermal resistances that characterise the heat transfer between the fluid in the condenser and external environment (cold source), and between the fluid in the accumulator and its external environment (intermediate source), respectively. Lastly  $R_g$  is the atypical thermal resistance, which takes in account the temperature difference connected with the pressure drop in the antigravity liquid line. It depends on the difference between the levels of the accumulator and condenser  $H$  and on the heat rate  $Q_m$ . In fact, considering that the working fluid inside the evaporator and the accumulator is at the saturation point, the pressure and temperature differences are linked by the Clausius Clapeyron equation:

$$p_{ev} - p_{acc} = \frac{(T_S(p_{ev}) - T_S(p_{acc})) \cdot r \cdot v_d}{\bar{T}} \quad (1)$$

where  $v_d$  is the differential volume at the mean temperature  $\bar{T}$  ( $\bar{T} = (T_{ev} + T_{acc})/2$ ) and  $r$  is latent heat of vaporization.

Considering also that the pressure difference between evaporator and accumulator is given by the relation:

$$p_{ev} - p_{acc} \geq \rho_l \cdot g \cdot H \quad (2)$$

where  $\rho$  is the density of the liquid,  $R_g$  can be expressed, if pressure losses are neglected, by the relation:

$$R_g = \frac{T_{ev} - T_{acc}}{Q_m} = \frac{\bar{T}}{r \cdot v_d} \cdot \frac{\rho_l \cdot g \cdot H}{Q_m} \quad (3)$$

After the definition of the single thermal resistance taken in account in a PTPT device, the total thermal resistance of a PTPT device can be calculated. In the simplest case of  $T_C = T_m$ , it is, therefore, given by the relation:

$$R_{PTPT} = R_B + \frac{R_C \cdot (R_g + R_m)}{R_C + R_g + R_m} \quad (4)$$

Usually a PTPT device is designed to transfer heat between evaporator and condenser so that  $Q \cong Q_C$  and  $Q_m$  is some order of magnitude lower than  $Q$ . Thus the thermal resistances  $R_g$  and  $R_m$  are extremely large and the PTPT total thermal resistance assumes the general form of:

$$R_{PTPT} = R_B + R_C = \frac{T_w - T_C}{Q} \quad (5)$$

The thermal behaviour of a PTPT is, therefore, determined by the heat transfer relative to evaporator heating surface and relative to the condenser, while is not influenced by the lifting liquid column height [8].

In order to drastically reduce the size of the evaporator without abruptly increasing the total thermal resistance, more attention must be paid to  $R_B$ , which have a large influence on the power rate dissipated by the device.

## Experimental procedure

In the experimental device the difference in levels between the evaporator and the accumulator and between the evaporator and the condenser remain constant throughout the tests and are equal to 0.5 m and 0.2 m (Fig. 1), respectively.

The experimental procedure starts with the loop evacuation ( $10^{-2}$  Pa) and its partial filling with working fluid.

With reference to the experimental condition, the mass of working fluid inside the loop is about 0.237 kg for a filling ratio of 40%, while the filling ratio of the evaporator is 59%.

After that the power input was supplied to the evaporator, the PTPT device started to operate and the volume of the liquid inside the evaporator completely evaporated, while in the accumulator was collected. As the evaporator is empty, a volume of cold liquid collected in the accumulator  $V_T$  had to be chosen to return to the evaporator. It is equal or lower than the starting volume of liquid inside the evaporator. The volume of the liquid  $V_T$  returning to the evaporator is indirectly given by the period where the electrovalves are opened  $\Delta\tau_2$  (ON), while the time where the electrovalves are closed  $\Delta\tau_1$  (OFF) is set in order to obtain a completely evaporation of the working fluid volume  $V_T$ . After the first transfer cycle (start up) the volume of liquid transferred  $V_T$  in the other cycles remains unchanged till a stable periodic heat transfer regime is reached. The volume  $V_T$  has been measured by the level meter inside the accumulator. As the stable periodic heat transfer regime was observed, the procedure has been repeated with a lower  $V_T$ .

All our tests have been carried out keeping the power input  $Q$  constant and decreasing  $V_T$  down to a minimum value that allowed a stable heat transport regime to be reached. The same procedure was repeated as the power input was increased. The power input was increased from  $5.1 \times 10^4$  W/m<sup>2</sup> (14 W) up to a heat flux of  $16.2 \times 10^4$  W/m<sup>2</sup> (45 W). For higher heat fluxes no stable heat transfer regime was observed.

On average, 4 different working fluid volumes  $V_T$  have been investigated for every power input, starting from a maximum value of about  $64 \times 10^{-6}$  m<sup>3</sup> up to values of about  $3 \times 10^{-6}$  m<sup>3</sup>.

## EXPERIMENTAL RESULTS

### Effect of the working fluid transferred volume

The aim of this paper is to observe the thermal behaviour of the evaporator as the volume  $V_T$  decreases. In particular, the minimum volume that makes it possible to reach a stable operating mode in a PTPT must be found if a drastic scale reduction of the device is required.

A decrease in the volume of working fluid transferred every cycle can influence the heat transfer regime close to the heating surface. As noted above the thermal resistance  $R_B$  connected with heat transfer between the heating surface and working fluid is very important to characterise the global thermal behaviour of the device.

The dimensions of the evaporator and heating surface (Fig. 1) do not influence the heat transfer close to the surface. During a single cycle, pressure, wall superheat and volume of liquid inside the evaporator, however, change over time. Moreover, it is interesting to note that the volume of liquid  $V_{ev,l}$  at the starting and ending time of a single cycle  $\tau_0$  and  $\tau_2$  is exactly equal to  $V_T$ , but at the time  $\tau_1$  it falls to zero.

During a single cycle, therefore, different heat transfer regime are expected: transient boiling, nucleate boiling, film boiling and vapour convective heat transfer.

Some qualitative considerations on the heat transfer regime experimentally observed over time can be made with reference to the trends of the temperatures  $T_w$  and  $T_s$  and its difference ( $T_w - T_s$ ) show in Fig. 4. The experimental data of

Fig. 4 are relative to a heat flux of  $14.44 \times 10^4 \text{ W/m}^2$  and a transferred volume  $V_T$  of working fluid of about  $64 \times 10^{-6} \text{ m}^3$ .

The wall superheat trend in a single cycle has been divided into 6 parts. The firsting part A is characterised by a sudden fall in wall superheat because the temperature  $T_W$  decreases while  $T_S$  increases. The reason why  $T_S$  increases is because the saturation pressure must reach the value needed to lift the condensed liquid to the accumulator, as described earlier. In part A all the transported volume  $V_T$  is inside the evaporator.

In part B the copper dissipator continues to give its accumulated heat to the fluid that uses it to evaporate by keeping its temperature  $T_S$  constant. This part is characterised by a transient heat transfer regime and the volume of liquid pool  $V_{ev,l}$  decreases. If the starting volume  $V_T$  is large, the dissipator reaches a steady state wall temperature during part A, and part B is not present in the qualitative trend; otherwise part B takes up a large portion of heat transport cycle. In Fig. 4, for example, part B is very small because it is referred to a large starting working fluid volume, but it is large as the volume  $V_T$  decreases as shown in Fig. 6, where the qualitative trend of the wall superheat at  $V_T$  is presented.

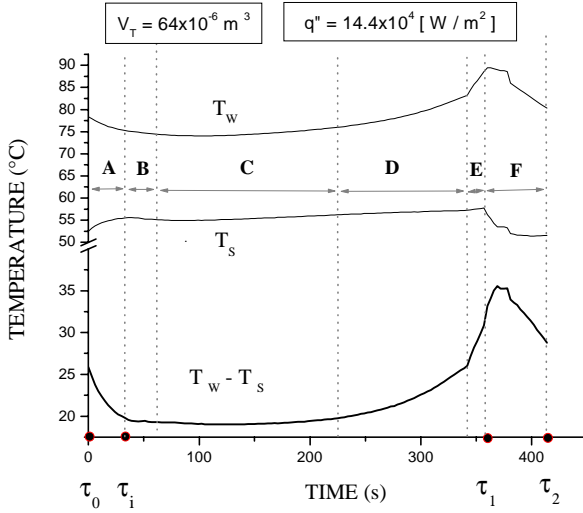


Fig. 4: Trends of the temperatures  $T_W$  and  $T_S$  and the wall superheat ( $T_W - T_S$ ) for  $14.44 \times 10^4 \text{ W/m}^2$

During part B the wall superheat tends to a constant value that we suppose to be determined by a steady state nucleate boiling regime, that is obtained in part C. In part C, in fact, the wall superheat, together to all the other parameters, remains unchanged, except for the volume of liquid pool  $V_{ev,b}$  which falls. In part E the volume  $V_{ev,b}$  reaches zero, and the heating surface is now in direct contact with the fluid vapours.

Part D is characterised by an heat transfer regime intermediate between the steady state nucleate boiling regime of part C and the transient convective heat transfer of part E. This effect on the heat transfer coefficient can depend on the only parameter that changes in part D, which is the volume of the pool  $V_{ev,l}$  inside the evaporator. This observation promotes the hypothesis that there is a minimum critical volume of the pool, for each heat flux, that makes it possible to obtain a steady state nucleate boiling regime. If the volume of the pool is lower than this value, a heat transfer coefficient lower than the boiling coefficient should be expected.

Lastly, in part F the return of the cold liquid on the heating surface occurs. Part F starts with the opening of the valves and finishes with their closing. The saturation pressure of the

working fluid inside the evaporator decreases because the cold liquid returns from the accumulator. The wall temperature  $T_W$  reaches its maximum value some seconds after the opening of the valves and this delay is due to the thermal inertia of the evaporator.

If  $V_T$  is lower than a critical value that depends on the heat flux, a steady state boiling regime is never obtained and the heat transfer coefficient is lower than the expected one, as can be seen from Fig. 5, where the wall superheat is presented at different transferred volumes of working fluid.

All the depicted trends of Fig. 5 show that the transient regime and phenomena connected with the thermal inertia of the evaporator become important as volume  $V_T$  decreases. For  $V_T$  lower than  $64$  to  $3 \times 10^{-6} \text{ m}^3$  no steady state boiling regime, characterised by a plate trend of the wall superheat (part C, Fig. 4), is obtained. The average heat transfer coefficients are therefore lower than the steady state boiling coefficients as the transferred volume of working fluid decreases.

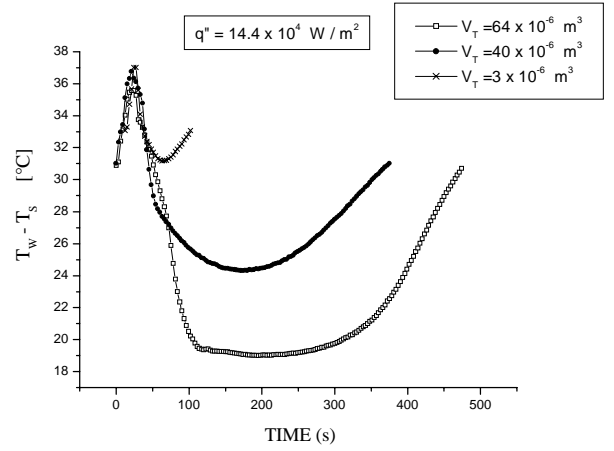


Fig. 5: Trends of the wall superheat  $T_W - T_S$  for  $10.8 \times 10^4 \text{ W/m}^2$  at different  $V_T$ .

The effect of the reduction in liquid volume inside the evaporator over time for a single cycle has been also considered measuring the transient heat transfer coefficient  $h_B$  on the heating surface, shown in Fig. 6. The transient heat transfer coefficient  $h_{B_{n+1}}$  at the time step number  $\tau_{n+1}$  has been calculated according to the following relation:

$$h_{B_{n+1}} = \frac{(q'' \cdot S \cdot (\tau_{n+1} - \tau_n) - M \cdot c_p \cdot (T_{W_{n+1}} - T_{W_n}))}{S \cdot (T_{W_{n+1}} - T_{S_{n+1}}) \cdot (\tau_{n+1} - \tau_n)} \quad (6)$$

where  $M$  and  $c_p$  are the mass and the specific heat of the copper dissipator, respectively, while  $q''$  is the heat flux and  $S$  is the heating surface. The time step is 3 s. The experimental data employed to obtain the heat transfer coefficients of Fig. 6 refer to the same conditions of the single cycle of Fig. 4.

As depicted in Fig. 6, part C of the heat transfer coefficient trend is almost constant and it has values similar to those for nucleate boiling regime [23], [24]. The other parts are characterised by transient heat transfer determined from an increase and a decrease in wall superheat with rates of 0.5 K/s and 0.35 K/s, respectively.

If is true that for volumes lower than a critical value no steady state boiling regime has been observed for a given heat flux, a stable periodic regime has been however obtained for very small transferred volumes of working fluid  $V_T$ . A quantitative analysis of the thermal resistances as  $V_T$

decreases has been carried out experimentally, and the results are reported in Table 1 for some dissipated heat fluxes.

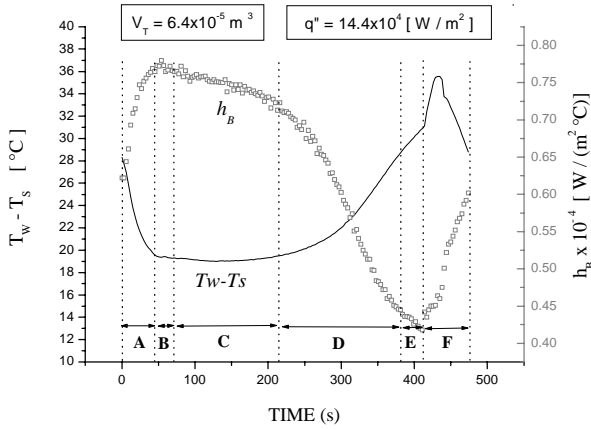


Fig. 6: Trends of the transient heat transfer coefficient

| $q'' \times 10^{-4}$<br>[ $\frac{W}{m^2}$ ] | $V_T \times 10^6$<br>[ $m^3$ ] | $\Delta \bar{T}_{(w-s)}$<br>[ $^{\circ}C$ ] | $\bar{T}_W$<br>[ $^{\circ}C$ ] | $T_{W \max}$<br>[ $^{\circ}C$ ] | $\bar{R}_T$<br>[ $\frac{K}{W}$ ] | $\bar{R}_B$<br>[ $\frac{K}{W}$ ] | $\Delta \tau_{tot}$<br>[s] |
|---|--------------------------------|---|--------------------------------|---------------------------------|----------------------------------|----------------------------------|----------------------------|
| 5.1   | 25                             | 15.45                                       | 56.9                           | 64.5                            | 2.87                             | 1.09                             | 858                        |
| 7.2   | 30                             | 20.76                                       | 66.5                           | 76.4                            | 2.44                             | 1.04                             | 963                        |
| 8.7   | 25                             | 27.02                                       | 66.3                           | 70.8                            | 1.99                             | 1.12                             | 225                        |
| 9.4   | 25                             | 28.61                                       | 67.3                           | 71.2                            | 1.93                             | 1.10                             | 204                        |
| 10.1  | 25                             | 32.09                                       | 72.2                           | 75.9                            | 1.90                             | 1.15                             | 183                        |
| 10.8  | 25                             | 35.44                                       | 72.9                           | 76.3                            | 1.83                             | 1.18                             | 156                        |
|   | 9                              | 36.04                                       | 80.2                           | 81.9                            | 2.03                             | 1.20                             | 129                        |
|   | 3                              | 37.33                                       | 84.5                           | 85.7                            | 2.17                             | 1.25                             | 69                         |
|   | 1                              | 39.25                                       | 87.9                           | 88.1                            | 2.29                             | 1.31                             | 33                         |
| 11.6  | 25                             | 36.42                                       | 74.9                           | 79.8                            | 1.74                             | 1.13                             | 141                        |
| 12.3  | 25                             | 36.64                                       | 78.1                           | 81.9                            | 1.72                             | 1.08                             | 153                        |
| 13.0  | 25                             | 38.92                                       | 78.7                           | 82.1                            | 1.68                             | 1.08                             | 147                        |
| 13.7  | 25                             | 44.95                                       | 81.7                           | 85.1                            | 1.69                             | 1.18                             | 103                        |
| 14.4  | 64                             | 23.60                                       | 79.2                           | 89.2                            | 1.47                             | 0.59                             | 492                        |
|   | 45                             | 27.92                                       | 82.1                           | 88.7                            | 1.56                             | 0.70                             | 381                        |
|   | 25                             | 48.71                                       | 85.1                           | 87.5                            | 1.65                             | 1.22                             | 96                         |
|   | 3                              | 49.46                                       | 90.3                           | 93.3                            | 1.81                             | 1.24                             | 90                         |
| 16.2  | 35                             | 37.12                                       | 88.2                           | 90.3                            | 1.55                             | 0.82                             | 162                        |
|   | 30                             | 39.92                                       | 88.4                           | 91.1                            | 1.55                             | 0.89                             | 162                        |
|   | 3                              | 42.98                                       | 96.7                           | 98.1                            | 1.74                             | 0.96                             | 81                         |

Table 1: Experimental results

From the experimental data reported in Tab. 1 it can be seen that a stable heat transport regime has been reached even with  $V_T$  of about  $3 \times 10^{-6} m^3$  together to maximum wall temperatures below  $100^{\circ}C$  up to heat flux of  $16.2 \times 10^4 W/m^2$ .

As noted above, a fall in the working fluid transferred volume leads to an increase in thermal resistance, if the heat flux remains unchanged. This increase is, however, small because it is less than 25% if  $V_T$  falls from 64 down to  $3 \times 10^{-6} m^3$ . This increase remains approximately unchanged at different heat fluxes.

In spite of the increase in thermal resistance, the amplitude of wall temperature oscillations decreases as the volume  $V_T$  of working fluid increases. This effect reduces the increase in thermal stress on the heating surface and limits the negative effect of the increase in thermal resistance.

It is possible to conclude that a drastic scale reduction in the volume  $V_T$  and, therefore, in the volume of evaporator, can be achieved. The minimum volume of working fluid  $V_T$  that makes possible a stable periodic together with good PTPT thermal resistances, is about  $3 \times 10^{-6} m^3$ .

### Periodic pool boiling regime

As hypothesised above, if the transferred volume of working fluid is higher than critical value relative to a given heat flux, in a long period of a single heat transfer cycle, an infinite flat surface boiling coefficient can be measured. This condition is repeated for every cycle, so that a periodic pool boiling regime should be maintained. But can this particular heat transfer regime be considered a stable periodic pool boiling regime or must it be considered a transient boiling regime, with the heat transfer coefficients lower than the expected ones?

In order to answer this question the experimental data have therefore been compared with data reported in literature relative to nucleate boiling heat transfer for an infinite flat surface with FC72 as working fluid. Moreover, the experimental data have been compared with some of the correlations used to predict the nucleate boiling heat transfer coefficients. However, some preliminary considerations must be made about the wall superheat and how it has been determined from our experimental data. In Fig. 7 the wall superheat has been plotted against time during the start up of the PTPT device for different heat fluxes. The wall superheat presents a periodic trend that is approaching a stable periodic regime.

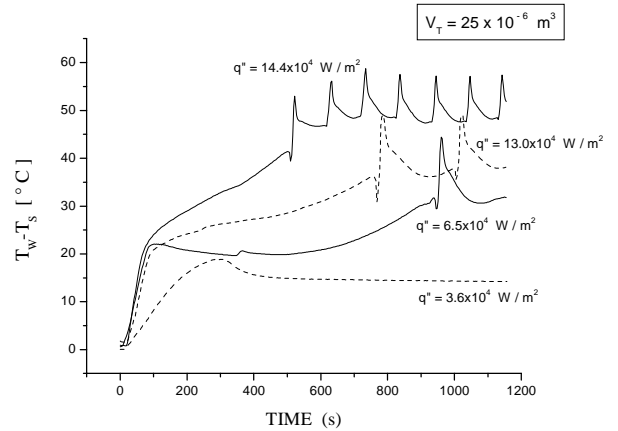


Fig. 7: Start up for different heat fluxes ( $V_T = 2.5 \times 10^{-6} m^3$ ).

For every cycle, as noted above, there is a part where a steady state boiling regime is expected (part C, Fig. 4). It has been supposed that this condition is realised as the wall superheat remains unchanged over time (when rises or falls in the rate are lower than  $0.015 K/s$ ). The numbers of time steps where this condition is true (part C lasting) decreases as the heat flux increases (Fig. 5). The wall superheat so determined and the relative heat flux measured have been compared with the experimental data and correlations in literature. It is important to note that the wall superheats relative to specific heat flux have been measured under different saturation pressures, while the data in literature are referred to a constant saturation pressure. In the PTPT device in fact the saturation pressure inside the evaporator depends on the heat flux. The

saturation pressure increases from 0.4 to 1.1 bar as the heat flux increases from  $5.1 \times 10^4$  to  $16.2 \times 10^4$   $\text{W/m}^2$ ).

The experimental data obtained by the elaboration have been compared with several correlations in order to predict nucleate boiling coefficients under different pressures. These correlations are: Rohsenow's correlation [26] that You et al. [23] have just applied to FC72, obtaining a good agreement, Cooper's correlation, corrected by Palm et al. [25] to predict the effect of pressure in two-phase loop thermosyphons, and Gorenflo's correlation, which examines the influences of the main groups on the heat transfer boiling coefficient in the VDI Atlas method [27]. Nishikawa's correlation [28] has been used too.

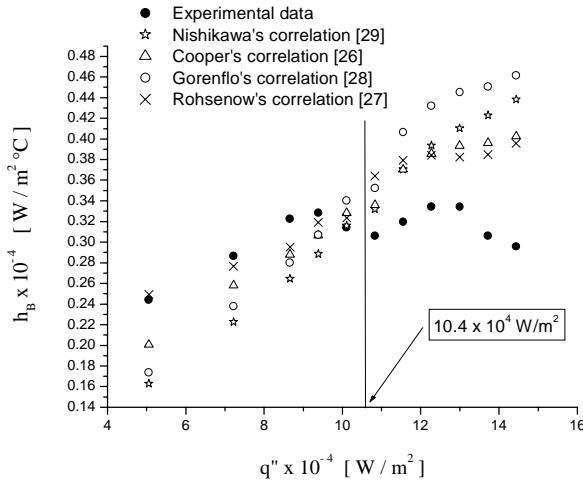


Fig. 8: Experimental data compared with the main correlation on nucleate boiling heat transfer.

The results of this comparison appear in Fig. 8. The correlation that has the best agreement with the experimental data is that of Rohsenow ( $C_{sf}=0.054$ ), which presents prediction errors lower than 9% for low fluxes, and higher than 13% for high fluxes. Cooper's correlation presents errors lower than 9% for heat fluxes lower than  $10.88 \times 10^4$   $\text{W/m}^2$  but higher errors (16%) in the opposite case. Similar results are obtained with the Gorenflo and Nishikawa correlations, which present errors lower than 13% and 15% for low heat fluxes and errors lower than 27% and 30% for high heat fluxes, respectively

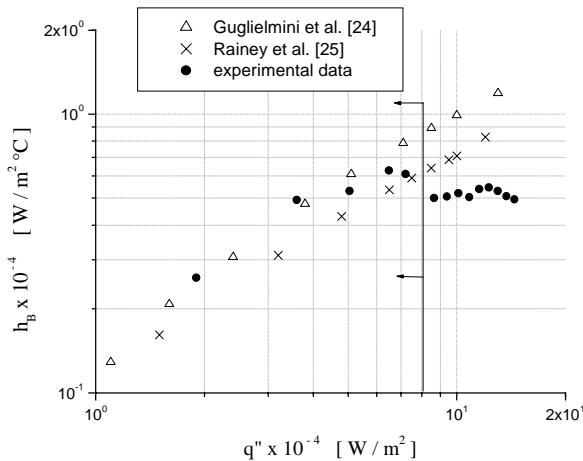


Fig.9: Experimental data compared with other results obtained with FC72 and  $p=1$  bar. Results appearing to the left of the vertical line show good agreement with boiling data.

Rohsenow's correlation has been used to correct the experimental data obtained under different pressures in order to compare them with those reported in [23], [24] relative to a constant saturation pressure of 1 bar. The results of this comparison are presented in Fig. 9.

From Fig. 8 and 9 it is clear that for high fluxes the heat transfer is not a steady state nucleate boiling. The maximum heat flux where the lower elaborated heat fluxes seem to show good agreement with the data in literature is about  $10.88 \times 10^4$   $\text{W/m}^2$ . By observing the changes in the qualitative trend of the wall superheat, it has been possible to measure the minimum volume  $V_{ev,l}$  required to obtain a steady state nucleate boiling regime. For a heat flux of  $10.88 \times 10^4$   $\text{W/m}^2$  the critical volume so measured is really  $25 \times 10^{-6}$   $\text{m}^3$ .

In conclusion the hypothesis of considering that the boiling heat transfer regime is obtained during a part of the heat transport cycle is really true if the  $V_T$  is higher than a critical value dependent on heat flux.

## CONCLUSIONS

In previous studies a miniature PTPT has been realised with an evaporator volume of  $238 \times 10^{-6}$   $\text{m}^3$ . It has shown thermal resistance similar to PHPs. These results seem to call for further investigation, but in order to use a PTPT device in microelectronic cooling the evaporator size must be drastically reduced. The volume of the evaporator in a PTPT device is connected with the minimum  $V_T$ . In this paper some experiments on the minimum volume  $V_T$  necessary to obtain a stable operating mode in a PTPT device are presented. The experimental results have shown that a stable heat transfer regime has been reached even with  $V_T=3 \times 10^{-6}$   $\text{m}^3$ . The maximum wall temperature remains below  $100^\circ\text{C}$  up to a heat flux of  $16.2 \times 10^4$   $\text{W/m}^2$ . A reduction in the volume  $V_T$  leads to an increase of thermal resistance, which is, however, smaller than 25% if  $V_T$  falls from  $64$  to  $3 \times 10^{-6}$   $\text{m}^3$ . The increase in thermal resistance is connected with the heat transfer regime in the evaporator. It has been observed that there is a critical volume in the liquid pool that allows a steady state boiling regime to be obtained. When the working fluid transferred volume is lower than this critical value, which depends on the heat flux, only transient boiling is observed. In this case the heat transfer coefficient is lower than that the expected one in a nucleate boiling condition. A further quantitative analysis of this dependence must be made in order to optimise the size of the evaporator.

## NOMENCLATURE

### Latin symbols

|          |                                  |                             |
|----------|----------------------------------|-----------------------------|
| $C_{sf}$ | Rosenhow's correlation coeff[28] | [dimensionless]             |
| $c_p$    | specific heat of the dissipator  | [J/kg]                      |
| $h$      | heat transfer coefficient        | [ $\text{W/m}^2 \text{K}$ ] |
| $H$      | level difference                 | [m]                         |
| $M$      | mass of the dissipator           | [kg]                        |
| $p$      | pressure                         | [Pa]                        |
| $Q$      | power input rate                 | [W]                         |
| $q''$    | heat flux                        | [ $\text{W/m}^2$ ]          |
| $r$      | latent heat of vaporization      | [J/kg]                      |
| $R$      | thermal resistance               | [K/W]                       |
| $S$      | heating surface                  | [ $\text{m}^2$ ]            |
| $T$      | temperature                      | [K]                         |
| $v_d$    | differential specific volume     | [ $\text{m}^3/\text{kg}$ ]  |

|                      |                      |                      |
|----------------------|----------------------|----------------------|
| V                    | working fluid volume | [m <sup>3</sup> ]    |
| <i>Greek symbols</i> |                      |                      |
| ε                    | emittance            | [dimensionless]      |
| ρ                    | density              | [kg/m <sup>3</sup> ] |
| τ                    | time                 | [s]                  |

#### *Subscripts*

|       |                                    |
|-------|------------------------------------|
| 1     | OFF time for electrovalves         |
| 2     | ON time for electrovalves          |
| acc,l | liquid in accumulator              |
| acc,v | vapour in accumulator              |
| B     | boiling                            |
| c     | cold source                        |
| ev,l  | liquid in evaporator               |
| ev,v  | vapour in evaporator               |
| g     | gravity                            |
| i     | isovolumic operation               |
| m     | intermediate source                |
| n     | time step counter                  |
| PTPT  | relative to the global device      |
| s     | saturation condition               |
| T     | transferred every cycle            |
| tot   | total (referred to a single cycle) |
| w     | wall                               |

#### REFERENCES

- Peterson G. P., *An Introduction to Heat Pipes, Modeling, Testing and Applications*, John Wiley & S., N.Y, 1994.
- Groll M. et al. Thermal Control of Electronic Equipment by Heat Pipes, *Rev. Gen. Du Therm*, vol. 37, 1998.
- Miyasaka A., Nakajima K., Tsunoda H., Experimental Results for Capillary Loop Pipe Applied to Direct Cooling Method, *J. Thermoph. Heat Tr.*, vol. 9, 1995.
- Khrustalev D. K., Semenov S. Y., Advances in Low Temperature Cryogenic and Miniature Loop Heat Pipes, *Proc. of 5th Minsk Seminar on Heat Pipes, Heat Pumps, Refrigerators*, Minsk, Belarus, 2003
- Maidanik Y. F. et al., Miniature Loop Heat Pipes for Electronics Cooling, *Applied Thermal Engineering*, vol. 23, pp 1125-1135, 2003.
- Rossi L., Polášek F., Thermal Control of Electronic Packaging by Heat Pipes and Two-phase Thermosyphons, *11th Int. Heat Pipe Conf.*, Tokyo, 1999.
- Khrustalev D., Loop Thermosyphon for Cooling of Electronics, Thermacore Inc. Notes, 2002.
- Fantozzi F., Filippeschi S., Latrofa E., Upward and Downward Heat and Mass Transfer with Miniature Oscillated Loop Thermosyphons, *Proc. 75 Eurotherm Sem., Micro Heat Transfer 2*, Reims, 2003.
- Akachi H., Polášek F., Štulc P., Pulsating Heat Pipes, *5th Int. Heat Pipe Symp.*, Melbourne, pp 208-217, 1996.
- Shafii M. B., A. Faghri, Y. Zhang, Thermal modeling of unlooped and looped pulsating heat pipes, *ASME J.Heat Transfer*, vol. 123, pp.1159-1172, 2002.
- Khandekar S., Groll M., An Insight into Thermo-Hydraulic Coupling in Pulsating Heat Pipes, *Int. J. of Thermal Science*, Elsevier Science, 2003.
- Rittidech S., et al., Correlation to Predict Heat and Transfer Characteristics of a Closed-End Oscillating Heat Pipe at Normal Operating Condition, *Appl. Therm. Eng.*, vol. 23, pp. 498-510, 2003.
- Fantozzi F., Filippeschi S., Pulsated Two-Phase Thermosyphons for Electronic Equipment Thermal Control, *Proc. 32 Int. Conf. On Env. Syst.*, San Antonio, 2002.
- Fantozzi F. et al., Heat Transport Device Based on Pulsing Thermosyphons with Forced Fluctuations of Pressure, *Proc. 12 Int. Heat Pipe Conf.*, Moscow, 2002.
- Sasin V. J. et al., Development and Research of a Two-Phase Pumpless Heat Transport System, *Proc. 2 Russian National Heat and Mass Conf.*, Moscow, 1998.
- Filippeschi S., Two Phase Thermosyphons Operating Against Gravity, Summary of PhD Thesis, University of Pisa, Italy, 2001.
- Tamburini P., T-System Proposal of a New Concept Heat Transport System, *3rd IHPC*, Palo Alto, 1978.
- De Beni G., Thoma H., Veneroni R., Friesen R., Device for Passive Heat Transport, UK PA n°8124363, 1983.
- Sasin V. J. et al. "Experimental Investigation and Analytical Modelling of Autoscillation Two-Phase Loop", *Proc. 9th IHPC*, Albuquerque, 1995.
- Fantozzi F., Filippeschi S., Latrofa E., Miniature Pulsated Loop Thermosyphon for Desktop Computer Cooling: Feasibility Study and First Experimental tests, *Proc. 5th Sem. Heat Pipes, Heat Pumps, Refr.*, Minsk, Belarus, 2003.
- Khrustalev D., Faghri A., Thermal Characteristics of Conventional and Flat Miniature Axially-Grooved Heat Pipes, *Journal of heat Transfer*, vol. 117, 1995.
- Zaghdoudi M. C., Tantolin C., Godet C., Flat Heat Pipe Thermal Performance in Body Force Environment, *ITHERM Proc. Intersociety Conf. on Thermal Phenomena, IEEE Conference*, Las Vegas, 2000.
- Guglielmini G., Misale M., Schenone C., Boiling of saturated FC-72 on square pin fin arrays, *Int. J. of Thermal Science 41*, Elsevier Science, 2002.
- Rainey K. N. et al., Effect of pressure, subcooling, and dissolved gas on pool boiling heat transfer from microporous, square pin-finned surfaces in FC-72, *Int. J. of Heat and Mass Transfer*, vol 46, pp. 23-35, 2003.
- Khobadandeh H., Palm B. Influence of System Pressure on the Boiling Heat Transfer Coefficient in a Closed Two-Phase Loop, *Int. J. Therm. Sci.*, vol .41, 2002.
- Rohsenow W. M., Hartnett J. P., *Handbook of Heat Transfer*, Mc Graw Hill Inc., ISBN 0070535760, 1973.
- Gorenflo D., State of Art in Pool Boiling Heat Transfer of New Refrigerants, *Int. J. Refr.*, vol. 24, pp. 6-14, 2001.
- Nishikawa K., Fujita Y., Ohta H., Hidaka S., Effect of the Surface Roughness on the Nucleate Boiling Heat Transfer over the Wide Range of Pressure., *Proc. 7 Int. Heat Transfer Conf., Munchen*, vol. 4., pp. 61-66, 1982.